Bioorganic & Medicinal Chemistry 19 (2011) 4882–4886

Contents lists available at ScienceDirect

Bioorganic & Medicinal Chemistry

journal homepage: www.elsevier.com/locate/bmc

Effects of β-glucosidase hydrolyzed products of harpagide and harpagoside on cyclooxygenase-2 (COX-2) in vitro

Liuqiang Zhang [a], Li Feng [a], Qi Jia [a], Jinwen Xu [b], Rui Wang [a], Zhengtao Wang [c], Yingchun Wu [a], Yiming Li [a,*]

[a] School of Pharmacy, Shanghai University of Traditional Chinese Medicine, 1200 Cailun Road, Shanghai 201203, China
[b] Murad Research Institute for Modernized Chinese Medicine, Shanghai University of Traditional Chinese Medicine, Shanghai 201203, China
[c] Institute of Chinese Materia Medica, Shanghai University of Traditional Chinese Medicine, Shanghai 201203, China

ARTICLE INFO

Article history:
Received 23 May 2011
Revised 23 June 2011
Accepted 23 June 2011
Available online 29 June 2011

Keywords:
Harpagide
Harpagoside
Iridoids
Anti-inflammation
β-Glucosidase
COX-2 inhibitors

ABSTRACT

Harpagide (**1**) and harpagoside (**2**) are two iridoid glycosides existing in many medicinal plants. Although they are believed to be the main bioactive compounds related to the anti-inflammatory efficacy of these plants, the mechanisms of their anti-inflammatory activities remain unclear. The results of our present study showed that **1** and **2** had no effects on inhibitions of cyclooxygenase (COX)-1/2 enzyme activity, tumor necrosis factor-α (TNF-α) release, and nitric oxide (NO) production in vitro. However, the hydrolyzed products of **1** and **2** with β-glucosidase treatment showed a significant inhibitory effect on COX-2 activity at 2.5–100 μM in a concentration-dependent manner. Our further study revealed that the hydrolyzed **2** product was structurally the same as the hydrolyzed **1** product (*H*-harpagide (**3**)). The structure of **3** was 2-(formylmethyl)-2,3,5-trihydroxy-5-methylcyclopentane carbaldehyde, with a backbone similar to prostaglandins and COX-2 inhibitors such as celecoxib. All of them have a pentatomic ring with two adjacent side chains. The result of molecular modeling and docking study showed that **3** could bind to the COX-2 active domain well through hydrophobic and hydrogen-bonding interactions, whereas **1** and **2** could not, implying that the hydrolysis of the glycosidic bond of **1** and **2** is a pre-requisite step for their COX-2 inhibitory activity.

1. Introduction

Harpagide (**1**) and harpagoside (**2**) are naturally occurring iridoids found in many medicinal plants such as *Scrophularia ningpoensis*,[1] *Scrophularia buergeriana*,[2] and *Harpagophytum procumbens*.[3] These medicinal plants have been shown to exhibit a variety of biological activities and used as pharmaceutical products and dietary supplements for the treatment of inflammatory ailments, such as faucitis,[4] rheumatoid arthritis[5] and osteoarthritis.[6] In vitro and in vivo bioassays have revealed that plants rich in **1** and **2** possess significant anti-inflammatory activities.[7] **1** and **2** are believed to be the main bioactive compounds related to the anti-inflammatory efficacy of these plants.

The mechanisms of anti-inflammatory efficacies of **1** and **2** are not fully understood due to controversies in the existing data. There are studies reporting that **1** and **2** arrested the expression of COX-2 and its product PGE2;[8] suppressed lipopolysaccharide-induced iNOS and COX-2 expression through inhibition of NF-kappa B activation;[9] and inhibited the production of IL-1β, IL-6, and TNF-α in mouse macrophage cells.[10] Several other studies, however, showed that **1** and **2** had no effect on 5-LOX, iNOS, and LPS-induced TNF-α release,[8,11] and **2** could even cause a significant increase in the level of COX-2 expression.[12]

Our previous in vitro assay results (unpublished) showed that **1** had no effect on cyclooxygenase (COX)-1/2 enzymes, tumor necrosis factor-α (TNF-α) release, and nitric oxide (NO) production. Our further experiment indicated that they were not antioxidants, either.[13] Recently, Park et al reported that some iridoid glucosides (aucubin, catalpol, gentiopicroside, swertiamarin, geniposide, geniposidic acid and loganin) were hydrolyzed by β-glucosidase first to display their inhibitory effects on COX-1/-2 and TNF-α.[14] In this study, we attempted to clarify the bioactive form of **1** and **2** by exploring the structures of compounds derived from β-glucosidase hydrolysis of **1** and **2** and their anti-inflammatory activities.

2. Results and discussion

2.1. Identification of the structure of the hydrolyzed product of harpagide (*H*-harpagide (3))

The structure of **3** was established by spectroscopic data and references with **1**. The ESI-MS spectrum showed that the molecular weight of **3** was 202 Da. ^{1}H NMR spectrum of **3** contained the

* Corresponding author. Tel.: +86 21 51322191; fax: +86 21 51322193.
E-mail address: ymlius@163.com (Y. Li).

0968-0896/$ - see front matter © 2011 Elsevier Ltd. All rights reserved.
doi:10.1016/j.bmc.2011.06.069

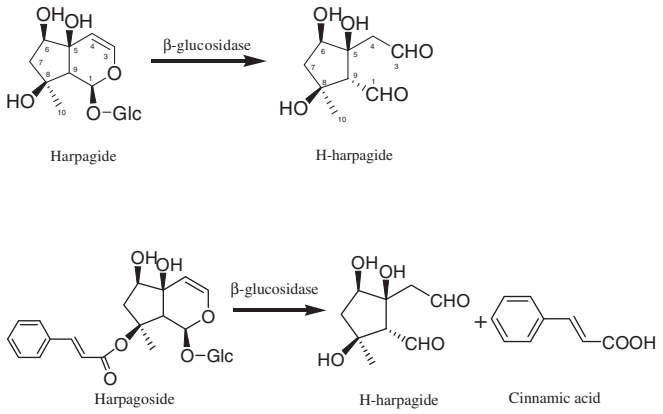

Figure 1. Hydrolysis reaction of **1** and **2** with β-glucosidase.

signals for two aldehyde protons, δ 10.16 (1H, s, H-1), δ 9.74 (1H, br s, H-3); a methyl group at δ 2.41 (3H, s, H-10) which linked to a quaternary carbon atom; three protons of ABX system δ 5.02 (1H, d, J = 6.6 Hz, H-6), δ 3.09 (1H, dd, J = 21.0, 6.6 Hz, H-7β), δ 2.78 (1H, d, J = 21.0 Hz, H-7α); two protons from multiple peaks at δ 2.33 (2H, m, H-4). By comparing the spectral data of **1**, the structure of **3** was readily deduced as 2-(formylmethyl)-2,3,5-trihydroxy-5-methylcyclopentane carbaldehyde (Fig. 1).

2.2. Effects on cell viability

No significant cytotoxicity on RAW 264.7 macrophages was observed for **1**, **2** and **3** at the concentrations observed (2.5–100 μM).

2.3. Effect on activities of COX-1/2 enzymes

The effects of **1**, **2**, and **3** on ovine COX-1 and human recombinant COX-2 were compared. The COX-1 or COX-2 derived prostanoid product was determined via enzyme immunoassay (EIA) using a broadly specific antibody that bound to all the major prostaglandin compounds. The background was detected with inactivated enzymes, and the value was 2.8 ± 0.5 for COX-1 and 2.9 ± 0.2 ng/ml and for COX-2. The enzyme 100% initial activity was determined by treated the enzyme with vehicle (DMSO), and the corresponding value was 45.7 ± 6.3 ng/ml for COX-1 and 152.0 ± 25.3 ng/ml for COX-2. Neither **1** nor **2** showed any inhibition on the two isozymes of COX at the concentrations 2.5–100 μM. The effect of **3** was also assayed (Fig. 2), showing that the product significantly inhibited the activity of COX-2 at concentrations 2.5–100 μM in a concentration-dependent manner with the value of IC_{50} 43.3 μM, and no inhibition for COX-1 was observed at the same concentration range. Aspirin and NS-398 were used as positive controls, which significantly inhibited COX-1 or COX-2 (P <0.01).

2.4. Effects on COX-2 mRNA expression in RAW 264.7 macrophages

The effects of **1**, **2**, and **3** on COX-2 mRNA expression in RAW 264.7 macrophages were determined by real-time PCR. No significant effect on basal mRNA expression of COX-2 was observed for the three compounds in RAW 264.7 cells at 20 and 100 μM. COX-2 mRNA expression was enhanced significantly by stimulation of LPS 1 μg/ml for 24 h (P <0.01) (Fig. 3). Compound **3** inhibited the LPS-enhanced COX-2 mRNA expression, with a maximal inhibition rate of 47.6% at 100 μM, but no inhibition was observed for **1** and **2** (data not shown). TPCK 20 μM inhibited COX-2 mRNA by 59.5%.

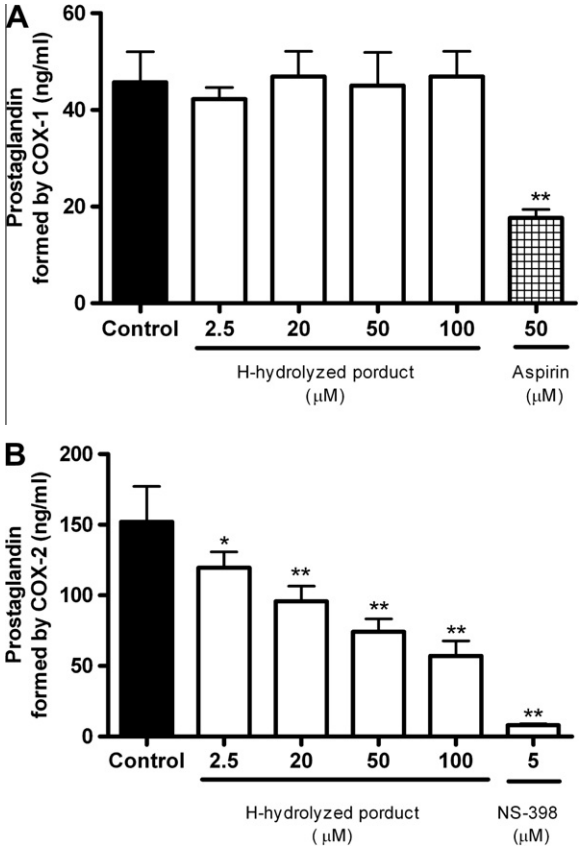

Figure 2. The effect of **3** on COX-1/2. The ovine COX-1 and human recombinant COX-2 were treated with vehicle (DMSO) or **3** for 10 min. The prostaglandins formed via COX-1/2 were determined by enzyme immunoassay (EIA). The values represented mean ± SEM. The enzymes treated with vehicle (DMSO) were used as control which represented enzyme 100% initial activity. The statistically significant difference $^{*}P$ <0.05, $^{**}P$ <0.01 compared with control. The data came from **3** independent experiments.

2.5. Effects on TNF-α formation and NO production in RAW 264.7 macrophages

Stimulation of RAW 264.7 murine macrophages by LPS resulted in production of large amounts of inflammatory substances including TNF-α and NO. Investigation of the effects of **1**, **2**, and **3** on RAW 264.7 cells treated with LPS showed that they had no inhibitory effect on the production of TNF-α and NO at the concentration range of 2.5–100 μM (data not shown), whereas the two positive drugs amino guanidine and dexamethasone showed a significant inhibitory effect on the production of NO and TNF-α.

2.6. Binding features of 3 with COX-1/2

The calculation results showed that the binding energy of **3** with COX-2 was lower than that of **1** or **2** with COX-2, **3** with the COX-1, which is consistent with the result of enzyme activity assay. The binding interactions of **3** with COX-2 and COX-1 could be simply described as hydrophobic interactions and hydrogen-bonding interactions.

2.6.1. Hydrophobic interactions

Figure 4A shows that **3** was surrounded by COX-2 residues Leu352, Tyr 387, Phe518,Val523, Gly526 and Ala 527 through hydrophobic interactions, which is consistent with the COX-2 inhibitor SC-558's. The hydrophobic interaction residues of COX-1 with **3** (Fig. 4B) were Val349, Leu352, Trp387, Phe518, Gly526,

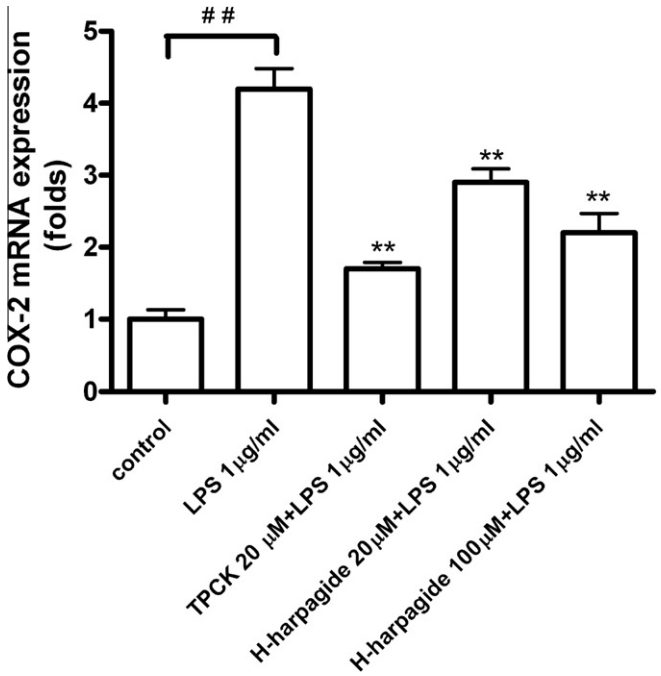

Figure 3. Effects of **1**, **2**, and **3** on COX-2 mRNA expression in RAW 264.7 macrophages. RAW 264.7 macrophages were pre-treated with **3** for 3 h, and then stimulated with LPS 1 μg/ml for 24 h. Total RNA was extracted and COX-2 mRNA expression was monitored by real-time PCR. The data were normalized with β-actin and expressed as the fold change in gene expression relative to the untreated cell group. All values were from **3** independent experiments and expressed as mean ± SEM versus control $^{\#\#}P$ <0.01 and LPS treated group $^{**}P$ <0.01. *N*-*p*-tosyl-L-phenylalanyl chloromethyl ketone (TPCK) 20 μM served as a positive control.

Ala527 and Ser530, which is also consistent with COX-1 inhibitor celecoxib on the whole. The hydrophobic interactions of **3** with COX-2 and COX-1 were relatively conservative to SC-558 and celecoxib.

2.6.2. Hydrogen-bonding interactions

Hydrogen bonding is an important characteristic of the interactions between **3** and COX-2. When bound to COX-2, **3** forms two hydrogen bonds with COX-2. Figure 4A shows clearly that the oxygen of **3** acts as a donor to form two hydrogen bonds with the hydroxyl group OH of Tyr385 and Ser530. Tyr 385 is known to be very important in keeping the catalysis activation of COX-2.[15] There was no hydrogen bond between **3** and COX-1, indicating that the inhibitory effect of **3** on COX-2 was stronger than that on COX-1.

2.7. Discussion

The above results indicate that **1** and **2** themselves did not show any anti-inflammatory efficacy in vitro. They are supposed to be in their active forms by enzymatic hydrolysis of glycosidic bond, leading to the *H*-iridoid products. Compound **1** was originally presumed to produce its aglycone after hydrolysis. However, the structure of the *H*-iridoid product of **1** was not just simple removal of sugar moiety to produce its aglycone form. Since the aldehyde acetal structure is not stable, the pyranoid ring of the aglycone was opened to form the dialdehyde structure of a new compound which exhibited an inhibitory effect on COX-2 and a suppressive effect on COX-2 mRNA expression. In the enzymatic hydrolysis process of **2**, the unstable aglycone would lose its cinnamic acid residue when the dialdehyde structure was formed. As a result, the structure of hydrolyzed products for **1** and **2** was the same.

Park et al. compared the anti-inflammatory effects of aucubin, catalpol, geniposide and loganin with their enzyme hydrolyzed-iridoid products (*H*-iridoid), and found that the glycosides themselves did not show any anti-inflammatory effects, whereas the hydrolyzed forms were bioactive. Although they presumed that the structures of *H*-iridoid products contained a cleavage of monoterpene rings, no related details were given.[14] In the present study, we purified **3** and determined its structure for the first time mainly based on NMR data. A closer look at the structure of **3** revealed an interesting finding that this structure somewhat looks like PGE2 or other COX-2 selective inhibitors, all of which have a pentatomic ring with two adjacent side chains. We think that the structural similarity to PGE2 makes **3** accessible to the active domain of COX-2 enzyme. This is probably the reason why **1** showed inhibition on COX-2 only after it was hydrolyzed and formed the pyranoid ring, and why **3** had no effect on TNF or iNOS. This observation may also help explain the result of Park et al. who found that genipin had no effect on inhibition of PGE_2 formation in LPS-stimulated RAW264.7 cells while *H*-geniposide was active on it. The enzymatic hydrolysis of geniposide produced an active form of aldehyde acetal, which was then easily transformed to a dialdehyde structure. However, genipin is stable and cannot be easily transformed to dialdehyde. *H*-gentiopicroside and *H*-swertiamarin were not effect on inhibition of PGE_2 formation either, since they cannot form a pentatomic ring; instead, they form a hexatomic ring with adjacent side chains, making it difficult to access the active domain of COX enzyme.

To further investigate the binding feature of **3** to COX-2, molecular modeling and docking were used. The modeling results provide a satisfactory explanation for the binding mode of **3** with COX-2. The predicted binding free energy of **3** with COX-2 was lower than that of 1/2 with COX-2, which is supported by the stronger hydrophobic interaction and existence of hydrogen bonds observed in the docking form of **3** to COX-2. All these results and observations offer a reasonable explanation of why the β-glucosidase hydrolyzed product of **1** is the active form to inhibition COX-2 effect.

3. Experimental

3.1. General experimental procedures

1 and **2** were isolated and purified from the roots of *Scrophularia ningpoensis* according to the method reported.[1] β-glucosidase (EC 3.2.1.21), 3-(4,5-dimethylthiazol-2-yl)-2,5-diphenyltetrazolium bromide (MTT), arachidonic acid (AA), lipopolysaccharide (LPS, from *Escherichia coli*, 011: B4), Aspirin, NS-398, aminoguanidine, *N*-*p*-tosyl-L-phenylalanyl chloromethyl ketone (TPCK), and dexamethasone were obtained from Sigma Chemical Co. (St Louis, MO, USA). Dulbecco's Modified Eagle's Medium (DMEM), fetal bovine serum (FBS), and other reagents for cell cultures were obtained from Gibco BRL Life Biotechnologies (Gaithersburg, MD, USA). The ^1H nuclear magnetic resonance (NMR) spectra were recorded on a Bruker Avance 600 spectrometer (Bruker, Faellanden, Switzerland).

3.2. Cell line

RAW 264.7 murine cell line was obtained from the Shanghai Institute of Cell Biology, Chinese Academy of Sciences (Shanghai, China), and maintained in media recommended by the supplier, supplemented with 10% FBS (Gibco, Paisley, UK), penicillin (100 U/ml) and streptomycin (100 μg/ml) in a humidified 5% CO_2 atmosphere at 37 °C.

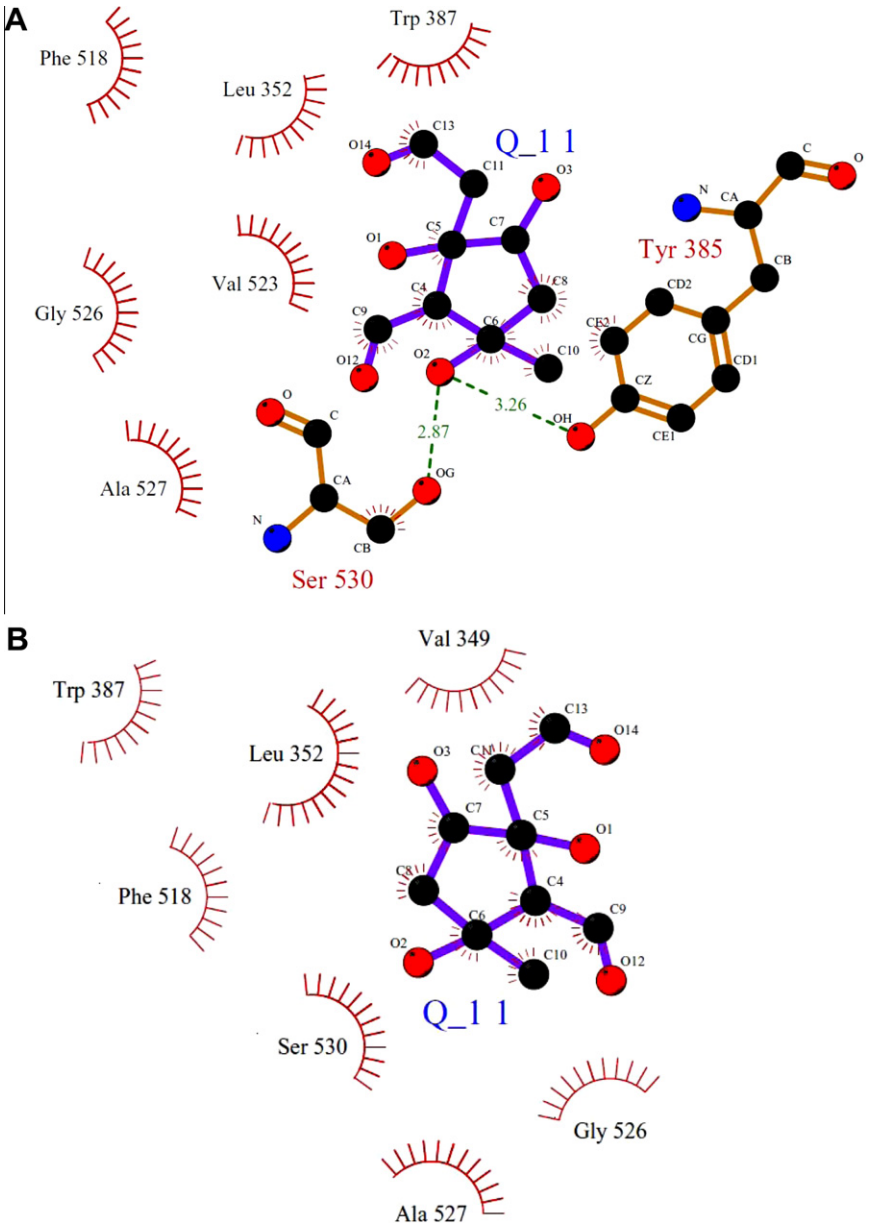

Figure 4. Hydrophobic interactions and hydrogen-bonding interactions of COX-2 with **3** (A) and COX-1 with **3** (B). The **3** atoms and the important residues for inhibitor–protein hydrophobic interaction are represented by pearlescent marks, respectively. Hydrogen bonds are depicted by green lines.

3.3. Hydrolysis of 2 or 1 with β-glucosidase

β-glucosidase was reported as an acid protease and stable at 50 °C. The reported optimal pH value for the hydrolysis was 4.8.[16] Here, the optimal hydrolysis conditions were established as: incubated **1** or **2** with β-glucosidase (5:1 w/w) in the acetic acid solution (pH 4) at 40 °C for 1 h. Compound **1** was checked and completely transformed into **3** by the TLC method (CH_2Cl_2–EtOAc 1:1). At the end of hydrolysis, the hydrolysis solution was extracted exhaustively with CH_2Cl_2 for three times. The combined CH_2Cl_2 solution was evaporated the solvent in vacuo at room temperature, and the residue was freeze-dried to get **3**. The properties of **3**: colorless powder, ESIMS (neg.) *m/z* 201 $[M-H]^-$; HRESIMS (neg.) *m/z* 201.0755 (calcd for $C_9H_{13}O_5$, 201.0759.); ^{1}H NMR ($CDCl_3$, 600 MHz), δ 10.16 (1H, s, H-1), 9.74 (1H, s, H-3), 2.33 (2H, m, H-4), 5.02 (1H, d, J = 6.6 Hz, H-6), 3.09 (1H, dd, J = 21.0, 6.6 Hz, H-7β), 2.78 (1H, d, J = 21.0 Hz, H-7α), 3.67 (1H, br s, H-9), 2.41 (3H, s, H-10).

Meanwhile, the hydrolyzed compounds of **2** were the same as **3** and cinnamic acid, as demonstrated by TLC and ^{1}HNMR.

3.4. Cell viability assay

RAW 264.7 murine macrophages were seeded into 96-well plates. After co-incubation with the compounds tested or vehicle for 18 h, 3-(4, 5-dimethylthiazol-2-yl)-2, 5-diphenyl tetrazolium bromide (MTT) was added to give a final concentration of 0.5 μg/ml. With addition of 100 μl DMSO to each well, cells were incubated for additional 4 h. The amount of formazan accumulated in the growth medium was assessed at 570 nm using a microplate reader.

Conditions were considered toxic if the ability of cells to metabolize MTT to formazan was more than 20% lower than that of the control.

3.5. Cyclooxygenase-1/2 (COX-1/2) assay

The effects of the compounds on COX-1/2 were determined with COX inhibitor screening assay kit (Cayman Chemical Company, Ann Arbor, MI, USA) according to the instruction of the kit. Briefly, test compound solution or solvent 20 μl, reaction buffer 950 μl, heme 10 μl, and COX-1 (ovine) or COX-2 (human recombinant) 10 μl were incubated for 10 min, and AA 10 mM 10 μl was added to initiate the reaction and incubated for 2 min at 37 °C. One molar of HCl, 50 μl was added to terminate the reaction, and the samples were then treated with 100 μl saturated stannous chloride solution for 5 min at room temperature. The activity of COX-1/2 was determined by quantification of prostanglandins formed with EIA.

3.6. RNA extraction and reverse transcription real-time quantitative polymerase chain reaction

The RAW 264.7 murine macrophages were seeded in six-well plates (2×10^5 cells per well) for RNA extraction. Cells grown to confluence were treated with the test compound solution or vehicle solution for 3 h, and then stimulated with LPS 1 μg/ml for 24 h. Total RNA was extracted using TRIzol reagent (Invitrogen Corporation, Carlsbad, CA, USA) according to the manufacturer's instruction. The cDNA reverse-transcribed from total RNA was subjected to real-time PCR using fluorescent dye SYBR Green and Thermal Cycler Dice Real time System TP800 (TaKaRa Bio Inc., Kyoto, Japan). The reagents used above were from SYBR PrimeScript RT-PCR Kit (TaKaRa Bio Inc., Kyoto, Japan). The COX-2 primers (Forward 5' TGTGCGACATACTCAAGC 3', Reverse 3' CTGATGCACGTTGTGGAC 5') were designed according to the corresponding reference sequences in the NCBI data base. PCR thermocycler conditions comprised an initial holding at 95 °C for 15 s and subsequently a two-step PCR programme consisting of 95 °C for 15 s and 60 °C for 1 min for 40 cycles. Each sample was determined in duplicate. The relative changes of mRNA between the test and control samples were quantitated using the 2-ΔΔCt method.[17] The data were normalized with β-actin and expressed as the fold change in gene expression relative to the untreated cell group.

3.7. Assay of TNF-a formation

RAW264.7 cells (2×10^5 cells/well) were pretreated with the test compounds, dexamethasone or vehicle solution for 30 min, and then co-incubated with LPS (100 ng/ml) for further 6 h. The TNF-α formed in supernatants was determined by ELISA (eBioscience, San Diego, USA).

3.8. Assay of NO production

RAW264.7 cells (2×10^5 cells/well) were pretreated with the test compounds, aminoguanidine or vehicle solution for 20 min, and then co-incubated with LPS (1 μg/ml) for further 18 h. Hundred microlitre supernatant was incubated with Griess reagent (50 μl 1% sulfanilamide and 50 μl 0.1% naphthylethylenediamine in 2.5% phosphoric acid solution). The absorbance at 570 nm was measured and referred to a standard curve of sodium nitrite solution to determine the nitrite concentration.

3.9. Statistics

Data were expressed as mean ± SEM. Statistical analysis of the data was performed by one way analysis of variances followed by Dunnett's test. Values of $P < 0.05$ were considered statistically significant.

3.10. Molecular modeling and docking

The crystal structure of COX-2 complexed with the inhibitor SC-558 (PDB ID:6COX) was downloaded from the RCSB protein data bank and the PDB ID of COX-1 complexed with the inhibitor celecoxib is 3KK6. The potential of the 3D structures of COX-2 was assigned with Kollman-united charges encoded in the molecular modeling software Sybyl 7.3 (Linux-os2x).The initial structures of **1** and **2** were recovered from PubChem Compound home (http://www.ncbi.nlm.nih.gov/pccompound). The structures of **3** and *H*-harpagoside were built by Chemdraw Ultra 7.0. Partial atomic charges were computed using Sybyl 7.3, applying Gasteiger-Marsili. For the purpose of tackling the interaction mode of the inhibitors with enzyme, the advanced docking program Autodock 3.0.3 was used to perform the automated molecular docking. All compounds of the training set were manually docked into the SC-558 (or celecoxib) binding pocket of the COX-2 (COX-1) enzyme.50 docked structures of the inhibitor were generated after a reasonable number of evaluations. Finally, the docked complexes of inhibitor-enzyme were selected according to criteria of interacting energy combined with geometrical matching quality.

Acknowledgements

This research program was supported by the National Science and Technology Major Project of China 2009ZX09103-398; the Program for Professors of Special Appointment (Eastern Scholar) in Shanghai Institutions of Higher Learning and the Program for Shanghai Key Discipline Establishment of TCM Pharmaceutics (J50302); the "Xinlin" scholars and outstanding team training plan of SHUTCM and the National Natural Science Foundation of China (No.81073027).

A. Supplementary data

Supplementary data associated with this article can be found, in the online version, at doi:10.1016/j.bmc.2011.06.069. These data include MOL files and InChiKeys of the most important compounds described in this article.

References and notes

1. Li, Y.; Jiang, S.; Gao, W.; Zhu, D. *Phytochemistry* **1999**, *50*, 101.
2. Lin, S.; Jiang, S.; Li, Y.; Zeng, J.; Zhu, D. *Tetrahedron Lett.* **2000**, *41*, 1069.
3. Qi, J.; Chen, J.; Cheng, Z.; Zhou, J.; Yu, B.; Qiu, S. *Phytochemistry* **2006**, *67*, 1372.
4. Jiangsu New Medical College. The Dictionary of Chinese Herb; Shanghai Science and Technology Press: Shanghai, 1977; Vol. 1, p. 769.
5. Cameron, M.; Gagnier, J. J.; Little, C. V.; Parsons, T. J.; Blümle, A.; Chrubasik, S. *Phytother. Res.* **2009**, *23*, 1647.
6. Chantre, P.; Cappelaere, A.; Leblan, D.; Guedon, D.; Vandermander, J.; Fournie, B. *Phytomedicine* **2000**, *7*, 177.
7. Chrubasik, J. E.; Roufogalis, B. D.; Chrubasik, S. *Phytother. Res.* **2007**, *21*, 675.
8. Ouitas, N. A.; Heard, C. M. *Int. J. Pharm.* **2009**, *376*, 63.
9. Huang, T. H.; Tran, V. H.; Duke, R. K.; Tan, S.; Chrubasik, S.; Roufogalis, B. D.; Duke, C. C. *J. Ethnopharmacol.* **2006**, *104*, 149.
10. Inaba, K.; Murata, K.; Naruto, S.; Matsuda, H. *J. Nat. Med.* **2010**, *64*, 219.
11. Fiebich, B. L.; Heinrich, M.; Hiller, K. O.; Kammerer, N. *Phytomedicine* **2001**, *8*, 28.
12. Abdelouahab, N.; Heard, C. *J. Nat. Prod.* **2008**, *71*, 746.
13. Li, Y.; Han, Z.; Jiang, S.; Jiang, Y.; Yao, S.; Zhu, D. *Acta Pharmacol. Sin.* **2000**, *21*, 1125.
14. Park, K. S.; Kim, B. H.; Chang, I.-M. *ECAM* **2010**, *7*, 41.
15. Kurumbail, R. G.; Stevens, A. M.; Gierse, J. K.; McDonald, J. J.; Stegeman, R. A.; Pak, J. Y.; Gildehaus, D.; Miyashiro, J. M.; Penning, T. D.; Seibert, K.; Isakson, P. C.; Stallings, W. C. *Nature* **1996**, *384*, 644.
16. Workman, W. E.; Day, D. F. *Appl. Environ. Microbiol.* **1982**, *44*, 1289.
17. Livak, K. J.; Schmittgen, T. D. *Methods* **2001**, *25*, 402.